ANNALS OF GEOPHYSICS, 68, 4, T445, 2025; doi:10.4401/ag-9276
OPEN ACCESS

Crustal Thermal Structures Modeling Using Temperature-Depth Profiles in Northern Thailand

Sorawat Siangpipop[1], Siriporn Chaisri[*,2], Niti Mankhemthong[1], Pisanu Wongpornchai[1]

(1) Chiang Mai University, Department of Geological Sciences, Chiang Mai, Thailand
(2) Chiang Mai University, Department of Physics and Materials Science, Chiang Mai, Thailand

Article history: received January 29, 2025; accepted July 24, 2025

Abstract

This study examines 1-D temperature-depth profiles (geotherms) in Northern Thailand by using computed compressional wave velocities (v_p) derived from shear wave velocities (v_s) models. These data, combined with various thermophysical parameters, are used to construct geotherms, focusing on thermal boundaries: the thermal brittle-ductile transition (thermal BDT), the thermal Curie point depth (thermal CPD), and the thermal uppermost mantle base (thermal lithospheric base). The study reveals relationships between geological boundaries, especially correlations between the depth of basin sediment-basement rock versus the thermal BDT and the upper-lower crust boundary versus the thermal CPD. The study also explores thermal BDT depth through crustal shear zone models based on frictional laws and quartzite flow assumptions. Additionally, assessing variability in crustal heat flow and strain rate informs understanding of crustal differential stress ($\sigma_3 - \sigma_1$). Beyond geological insights, the study of geothermal energy evaluates hot-dry rock (HDR) potential. The study also correlates the crustal thermal gradient with the locations of regional hot springs.

Keywords: Geotherm; Crustal Thermal Structure; Shear Zone Model; Geothermal Energy; Northern Thailand

1. Introduction

Northern Thailand (Fig. 1) reveals a fabric of intricate tectonic features and geological processes. This region is characterized by four primary tectonic terranes. These terranes, arranged from west to east, include the Sibumasu Terrane (ST), Inthanon Zone, Sukhothai Terrane, and Indochina Terrane (ICT). During the Late Paleozoic to Early Mesozoic, particularly throughout the Indosinian orogeny (Permian-Triassic), the ICT and ST underwent significant drifting and rifting from Gondwanan margins (Rozalli et al., 2020). This tectonic evolution facilitated the opening and subsequent closure of the Paleo-Tethys Ocean. The suturing of these terranes, especially between the ST and ICT, is recorded in the Inthanon Zone and Sukhothai Arc. Their collision and amalgamation resulted in crustal thickening and widespread magmatism by the Late Triassic (Hutchison, 2014; Zahirovic et al., 2014; Metcalfe, 2017). Subsequent tectonic reactivation during the Yanshanian orogeny (Middle to Late Jurassic-Early Cretaceous) and renewed deformation in the Cenozoic, particularly in relation to the Himalayan orogeny (starting ~50 Ma),

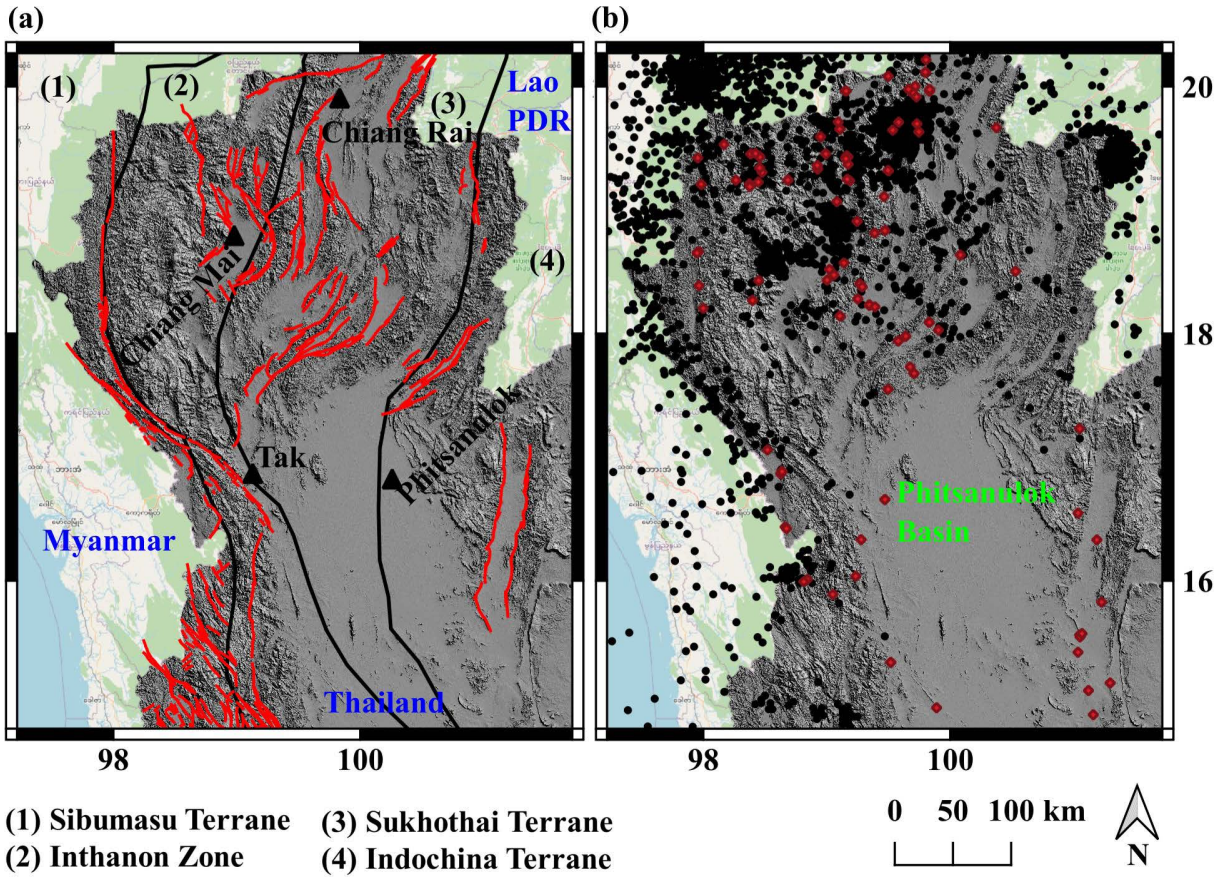

Figure 1. Map of study area, (a) black lines indicate terrane boundaries following Metcalfe (2017) and red lines show brittle shear zones following the Department of Mineral Resources (DMR, 2023b), (b) black dots show the epicenters of earthquakes with $0.6 \leq M_L \leq 6.3$ spanning from 2007 to 2021 by the Thai Meteorological Department (TMD, 2021) and hot spring locations by the Department of Mineral Resources (DMR, 2023a) are shown in red diamonds.

produced complex fault systems across the region. The ongoing India-Asia convergence has induced right-lateral displacements along NW-trending shear zones and left-lateral displacements along NE-trending faults (Charusiri, 2002). Today, Northern Thailand hosts 13 of the 16 active brittle shear zones mapped in the country, emphasizing its status as a seismically active region (DMR, 2023a).

Northern Thailand, with its complex geological features, has been the focus of extensive crustal-scale investigations aimed at understanding its tectonic evolution and geological structures. Seismological studies (Tadapansawut, 2012; Noisagool et al., 2014; Petkaew, 2015, 2022; Noisagool, 2022) have contributed to a comprehensive crustal exploration of this region. It is characterized by a relatively young, thin, and warm crust dominated by Triassic and younger rocks (Hansen and Wemmer, 2011; Hansen et al., 2014). The geological landscape is marked by suture zones and collision boundaries. The crust of Southeast Asia (SEA) exhibits high heat flow exceeding 75 $mW\,m^{-2}$ (Hall and Morley, 2004; Morley and Chantraprasert, 2022), and an average thermal gradient of 34.49 $°C\,km^{-1}$ (Jennings et al., 2021). However, thermal-structural studies have predominantly focused on near-surface temperatures through surveys (Wood et al., 2018; Uchida et al., 2011). This presents an opportunity to extend thermal investigations to a deeper scale for further insights into the region's thermal structure and geothermal potential.

The specific conditions, particularly steady-state and thermal equilibrium, contribute to the development of a 1-D temperature-depth profile, known as geotherm (Schettino, 2014). Geotherm offers significant means of approximating the temperature distribution within the conductive lithosphere (Chapman, 1986; Cull et al., 1991). It plays a pivotal role in thermal structures studies, especially where the mantle adiabat converges with the thermal lithospheric base at 1200-1300 °C (Artemieva and Mooney, 2001; Artemieva, 2006). Magnetic properties under varying temperatures define the Curie point depth (CPD), typically associated with magnetite at 400-600 °C (Okubo and Matsunaga, 1994; Tanaka et al., 1999). While the brittle-ductile transition (BDT) occurs between 150-500 °C, often linked to quartz-dominant composition (Caristan, 1982; Scholz 1988; Bonner et al., 2003).

The seismogenic zone is considered as the robust part of the lithosphere (Meyer et al., 2019; Stevens et al., 2021). The cutoff depth of crustal seismic hypocenters serves as a proxy for the seismogenic base, determined from the earthquakes catalogue using 95% confidence interval (Wu et al., 2017; Zuza and Cao, 2020). This boundary generally aligns with the BDT, marking the transition from brittle to ductile behavior (Nazareth and Hauksson, 2004; Fernández-Lozano et al., 2021; Lythgoe et al., 2021). Meanwhile, the CPD reflects the depth at which magnetite loses its magnetic properties (Dessai, 2020). The lithospheric base, crucial in understanding near-solidus rock behavior, is defined by the intersection of the geotherm with the thermal lithospheric boundary (Artemieva, 2011; Rychert et al., 2020).

This study focuses on interpreting thermal boundaries using estimated geotherms derived from two-layered crustal shear wave velocity (v_s) models representing crustal physical structures: sediment basement, upper crust, and lower crust, as presented by Siangpipop (2022). The v_s models are converted into compressional wave velocities (v_p) using data from Jackson and Arculus (1984). The calculated v_p, combined with existing observations (i.e., surface temperature, heat generation, measured heat flow, and measured thermal conductivity), along with relevant approximations, and laboratory data, serve as the foundation for estimating key thermophysical parameters to determine the crustal thermal structures. The conceptual crustal model, comparing the crustal physical structure and crustal thermal structure, is shown in Fig. 2.

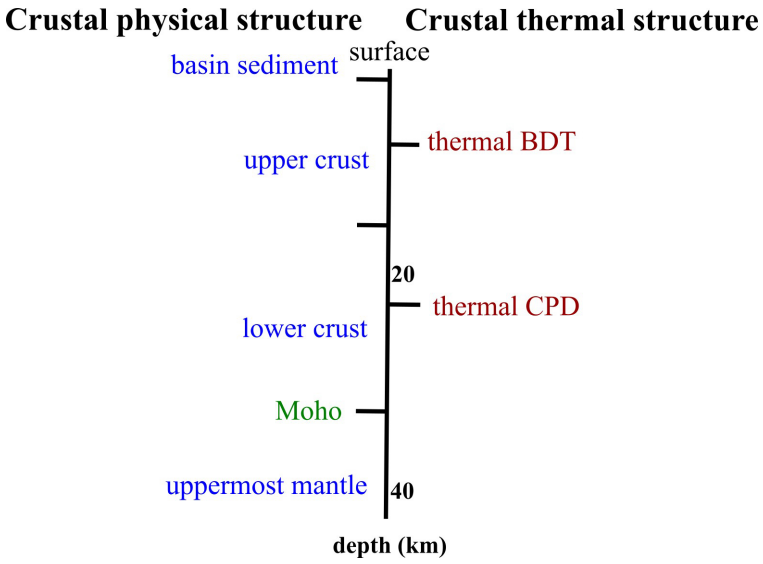

Figure 2. Conceptual crustal model, (left) crustal physical structures and (right) crustal thermal structures.

The genesis of earthquakes is linked to the geological structures and the deformation processes within shear zones under tectonic stress (Sibson, 1986). Shallow earthquakes are more influenced by brittle deformation through friction, and deeper regions are more prone to ductile deformation through viscous processes (Imber et al., 2001; Wehrens et al., 2016). A conceptual shear zone model suggests that seismic activity in upper brittle shear zone extends downward through a thermal-controlled transition, entering ductile shear zones (Price et al., 2012). The transition between the brittle and ductile segments is known as the BDT or frictional-viscous transition (FVT) (Imber et al., 2001; Wehrens et al., 2016). The shallow brittle segment can withstand greater stress than the underlying ductile crust (Behr and Platt, 2014). The shallow portion of models tends to be governed by the friction law, while the deeper section follows a steady-state flow law, often modelled using the quartzite flow law (Scholz, 1988; Fagereng and Toy, 2011). The BDT plays a pivotal role in seismic activity (Wright et al., 2013; Chiarabba and De Gori, 2016; Craig and Jackson, 2021; Lythgoe et al., 2021). A higher geothermal gradient or heat flow (hotter geotherm) elevates the BDT to relatively shallower depths compared to a lower heat flow (colder geotherm) (Behr and Platt, 2014; Zuza and Cao, 2020).

This study aims to compute average regional shear zone models to incorporate temperature and differential stress profiles in Northern Thailand. Previous examinations of major shear zones' rocks and associated structures are integrated for accounting a range of shear behaviors. Our models also consider the impact of variations in crustal heat flow and strain rate on the model's differential stress.

Beyond the geological implications, the studies address the growing energy demand in Thailand, emphasizing alternative energy sources. The national Alternative Energy Development Plan (AEDP) aims to increase the utilization of alternative energy sources to 30% by 2037 (MOE, 2018). Geothermal energy is integrated to this plan. Although traditional geothermal plants are well-established in Thailand, particularly in regions with abundant hot springs, such as those studied by Wood et al. (2018) in Northern Thailand, hot dry rock (HDR) presents a unique opportunity for future development.

The last section utilizes geotherms to assess the geothermal potential in Northern Thailand, particularly within the depth of basin sediment-basement rock and upper crust. Through geothermal analysis, such as estimating the theoretical stored heat content (Q_{block}) and approximating thermal energy, the study provides valuable insights into the potential for low-grade to high-grade HDR resources (Tester et al., 2006; Chamorro et al., 2014; Jiang et al., 2016; Aghahosseini and Breyer, 2020). Additionally, the thermal gradients are analyzed at reference depth, providing an initial indication of the main thermal sources for hot springs in the study area.

2. Thermophysical parameters

The crustal geotherm (T_z) is approximated using a 1-D partitioned geotherm equation:

$$T_z = T_0 + (q/k)\Delta z - (A/2k)\Delta z^2 \tag{1}$$

where T_0 represents the temperature at the top layer in K, q signifies the heat flow in mW m^{-2}, k denotes the thermal conductivity in W m^{-1}K^{-1}, A is the heat generation in μW m^{-3}, and Δz is thickness of the layer in km.

Through boot-strapping technique, the geotherm is calculated step by step for each 0.1 km increment. This process is conducted by cooperating with other parameters within each of the partitioned boundaries using v_s models in Fig. 3. The initial thermophysical parameters including the mean surface temperature, measured heat flow, and measured thermal conductivity, are necessary for the calculations. The mean surface temperature is obtained from the observation spanning from 2015 to 2019 by the Thai Meteorological Department (TMD, 2019). These data have been observed across each province (Fig. 4a). The interval of time is chosen to mitigate the influence of climate patterns. Notably, the study area's average surface temperature is recorded as 27.72 °C. The comprehensive dataset of 73070 measured heat flow values has been collected globally from https://ihfc-iugg.org/ (Thienprasert and

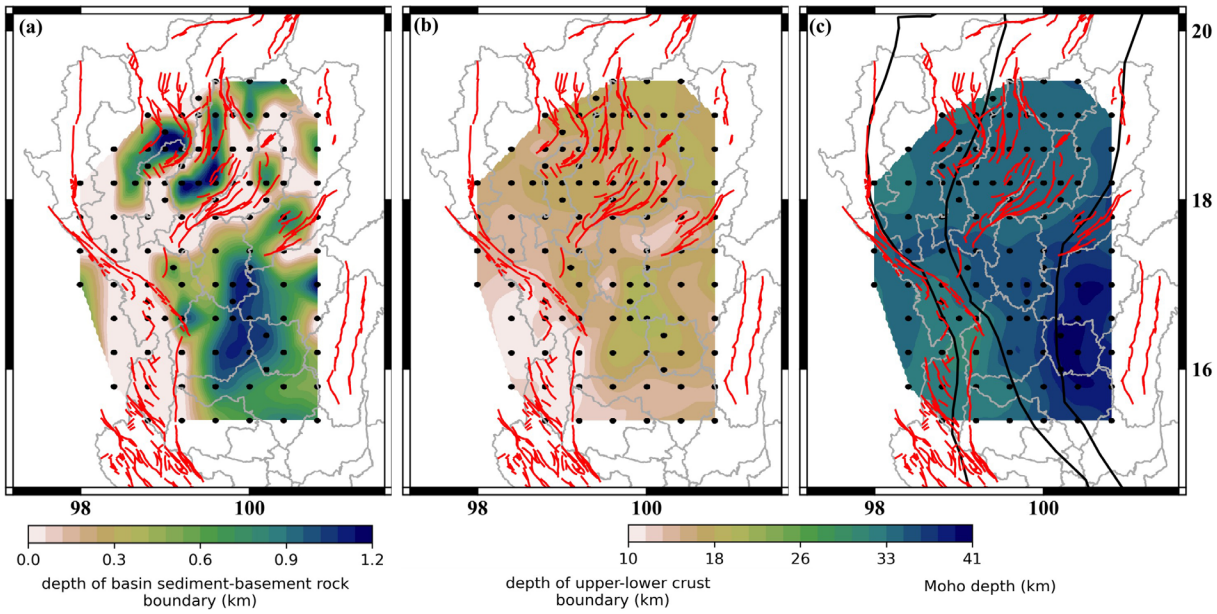

Figure 3. The depth boundaries obtained from v_s model by Siangpipop (2022), include (a) depth of basin sediment-basement rock, (b) depth of upper-lower crust boundary, and (c) Moho depth. The dots are inversion grid.

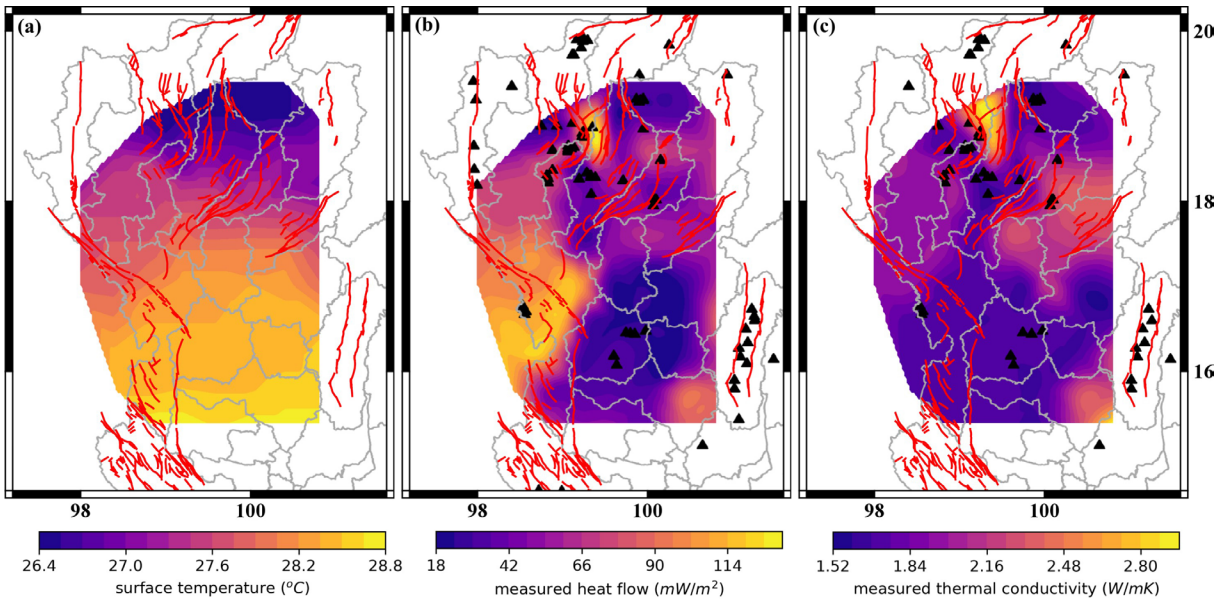

Figure 4. The initial thermophysical parameters mapped and overlaid the inversion grid. The surface temperature (a) from TMD (2019), the measured heat flow (b), and the measured thermal conductivity (c) from Thienprasert and Raksaskulwong (1984), Raksaskulwong and Thienprasert (1995), and Fuchs et al. (2023) with triangles indicate the available observation stations

Raksaskulwong, 1984; Lekuthai et al., 1995; Raksaskulwong and Thienprasert, 1995; Fuchs et al., 2023). Then, the interval range is constrained with a minimum of 20 $mW\,m^{-2}$ and a maximum of 130 $mW\,m^{-2}$ (Artemieva, 2011), while the off-limits values are suggested to be due to the potential environmental impacts from boreholes. Additional data points, particularly missing-data boundaries, were included based on tectonic provinces, as shown in Fig. 4b. The measured thermal conductivity is sourced from observation (Thienprasert and Raksaskulwong, 1984; Lekuthai et al., 1995; Raksaskulwong and Thienprasert, 1995; Fuchs et al., 2023), revealing a conductive range spanning from 1.68 to 2.76 $W\,m^{-1}K^{-1}$ in the region (Fig. 4c).

These recorded values were mapped onto the v_s model grid devised by Siangpipop (2022), and the application was carried out from the surface down to the depth of basin sediment-basement rock, or at least to the topmost 0.1 km of the considered weathered layer.

2.1 The estimation of thermal conductivity (k)

The sedimentary thermal conductivity is obtained from the observations (Fig. 4c). For crustal scale, since k is highly varying, the global-scale estimations are employed in this study. In the upper crust, which is relatively heterogeneous, k exhibits an inverse relationship with depth and temperature, resulting in a range of 3.0 – 2.055 $W\,m^{-1}K^{-1}$. Conversely, the lower crust is considerably much more homogeneous, leading to the assumption of a constant thermal conductivity value of 2.57 $W\,m^{-1}K^{-1}$. These values have been averaged from regions with high heat flow (rifts) and low heat flow (shields) as studied by Chapman (1986).

For the uppermost mantle, peridotitic rock, primarily composed of olivine, is adopted following Schettino (2014). A constant value of 4.0 $W\,m^{-1}K^{-1}$ has been assigned for mantle conductivity (Schatz and Simmons, 1972; Schärmeli, 1979).

2.2 The estimation of heat generation (A)

The determination of the heat generation for sedimentary basin A_s is highly unpredictable, due to the erosion and sedimentation. The A_s value is determined by using the formula from Rybach (1976) with the radiometric characteristics from the median value of color map by DMR (2018).

The crustal heat generation A_c is determined by using relationship presented in Rybach and Buntebarth (1984), which correlates A_c in $\mu W\,m^{-3}$ with v_p in $km\,s^{-1}$ as follows:

$$\ln A_c = 13.7 - 2.17 v_p \tag{2}$$

The conversion v_s to v_p by linear relationship derived from the study of Australian felsic to mafic granulite xenoliths conducted by Jackson and Arculus (1984). The assumption that Thailand's crust was once connected to the Australian continent underscores the interconnected geological history and shared characteristics between these regions.

However, it is important to note that the Eq. (2) was originally derived for a pressure of 100 MPa. To account for variations with depth, appropriate corrections must be applied. In this study, the upper crust is reasonably assumed to be granitic rock, and the lower crust is assumed to be granulitic rock in general (Cull et al., 1991; Hasterok and Chapman, 2011; Mareschal and Jaupart, 2013; Förster et al., 2021). Therefore, the v_p used for the upper crust is considered as 1.01 times the v_p from models. For the lower crust, the initial converted v_p from models is corrected with 0.99. This results in velocity ranges of 6.03-6.38 $km\,s^{-1}$ for the upper crust and 6.25-6.52 $km\,s^{-1}$ for the lower crust.

Moreover, the upper crust generally composed of radiogenic elements with heat generation exponentially decreasing with depth. Therefore, the heat generation in the upper crust needs to be corrected (Chapman, 1986) using the equation:

$$A(z) = A_0 \exp(-z/D) \tag{3}$$

where D is a constant characteristic of each heat flow province, A_0 represents the heat generation at the top layer, and z is depth in km.

As a result, an average heat generation of 1.07 $\mu W\,m^{-3}$ for the basin sediment has been estimated. In the upper crust, the average value is 0.95 $\mu W\,m^{-3}$, with depth variation described by Eq. (3). For the lower crust, an average constant value of 0.35 $\mu W\,m^{-3}$ is assigned. These values vary with grid locations due to differences of v_p. Heat generation in the uppermost mantle is negligible due to its comparatively small value (Mareschal and Jaupart, 2013).

2.3 The estimation of heat flow (q)

The crustal heat flow, including the sedimentary and weathered layers, is calculated using the basal heat flow of a layer (q_B) with the following relation:

$$q = q_B + AD. \tag{4}$$

The continental heat flow sources are approximately 40% from the radiogenic upper crust and 60% from deeper sources such as radioactive decay, advective processes, or heat released from the Earth's cooling interior (Pollack and Chapman, 1977; Chapman, 1986; Furlong and Chapman, 2013). The primary source of continental crustal heat flow is generally the radiogenic upper crust. Crustal heat flow decreases with depth, a concept known as basal or reduced heat flow (Chapman, 1986; Hasterok and Chapman, 2011; Förster et al., 2021).

Southeast Asia's crust is relatively young, dominated by Triassic and younger rocks, and characterized as thin and warm. The average thermal gradient of Thailand's onshore is 34.49 $°C\,m^{-1}$ (Jennings et al., 2021). These constraints were considered when selecting the q_B for our models.

A q_B value of 70 $mW\,m^{-2}$ has been reasonably adopted for the radiogenic upper crust using a trial-and-error approach. This value results in an average heat flow 85.27 $mW\,m^{-2}$ and thermal gradient 35.97 $°C\,km^{-1}$ for the radiogenic upper crust. This value ensures that the geotherms intersect the adiabat at 1200 °C. To evaluate the lower crust heat flow, mantle heat flow and heat generation (A) must be determined (Cull et al., 1991; Hasterok

and Chapman, 2011; Mareschal and Jaupart, 2013). In this study, for calculating lower crust heat flow, the q_B was assumed to be the minimum value of measured heat flow, as the mantle heat flow must be at least the minimum measured heat flow in the region. Maintaining this minimum value is also crucial, as a lower value would produce a geotherm that does not intersect the adiabat at 1200 °C.

These described values are applied individually to each partitioned depth layer: basin sediment, upper crust, lower crust, and uppermost mantle. The upper crust thickness, determined through prior research of Siangpipop (2022), reveals a maximum depth of about 19.87 km beneath the Phitsanulok Basin with the minimum thickness of 10.9 km in Western Thailand. The lower crust thickness ranges from 13.75 km to 23.8 km, increasfig. 5ng towards the southern part of the study area.

3. Crustal thermal structure

The determination of crustal thermal structures in Northern Thailand is essential for understanding geological processes and seismic activity. In this study, the seismogenic base is identified as the depth corresponding to the 95% confidence interval cutoff depth (D95) of earthquake events, sourced from the Thai Meteorological Department (TMD) regional earthquake catalogue spanning from 2007 to 2021 (TMD, 2021). Among the analyzed seismic events, 3205 events are considered shallow events (occurring 213.67 events yr^{-1}), while 85 events exceed the D95 of 10.2 km (occurring 5.67 events yr^{-1}), as shown in Fig. 5. The depth of 10.2 km aligns with the average geotherm temperature, resulting in a 360.5 °C isotherm for Northern Thailand. This temperature is presumed to signify the thermal point where assumed quartz-dominant composition begins to exhibit ductile behavior (thermal brittle-ductile transition, thermal BDT).

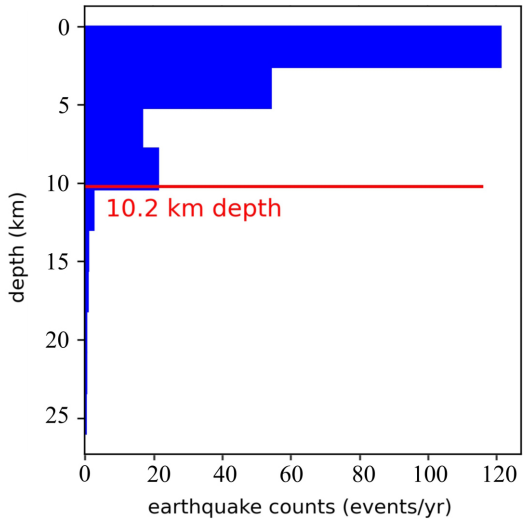

Figure 5. The number of earthquakes from 2007 to 2021, with local magnitude (M_L) 0.6-6.3 and their depths with red line separated shallow events and deep events (TMD, 2021).

The thermal Curie point depth (thermal CPD), occurring at 550 °C where magnetite loses its magnetic properties, closely corresponds to the elastic lithospheric base (Artemieva, 2011; Rychert et al., 2020). Moreover, the depth of CPD is generally shallower or equal to Moho depth, since magnetite is not stable in mantle. In addition, the thermal lithospheric base, characterized by the temperature near-solidus point of rock, is identified at 1200 °C.

To ensure result reliability, geotherms were initially compared with both the global thermal model (Artemieva, 2006) and SEA thermal model (Yu et al., 2017). Both models reveal a west-to-east thermal characteristic contrast, consistent with this finding.

From our thermophysical parameters estimation, the geotherms at each grid location are calculated and displayed in Fig. 6a. Our modeling domain is confined to the conductive region above the thermal lithospheric base. Geotherm segments extending beyond this boundary are excluded from subsequent calculations. The crustal physical structure

is derived from the average output of partitioned models across the study area, Fig. 6b. Figure 6c shows the crustal thermal structure with the thermal BDT at 360.5 °C and thermal CPD at 550 °C. To visualize the model output, Fig. 7 displays representative temperature distributions at depths of 10 km, 20 km and at the Moho depth.

Figure 8 displays all thermal boundaries based on the isothermal surface temperatures. The thermal BDT appears shallower in the southwest of the region, with the deepest thermal BDT observed in the Phitsanulok Basin.

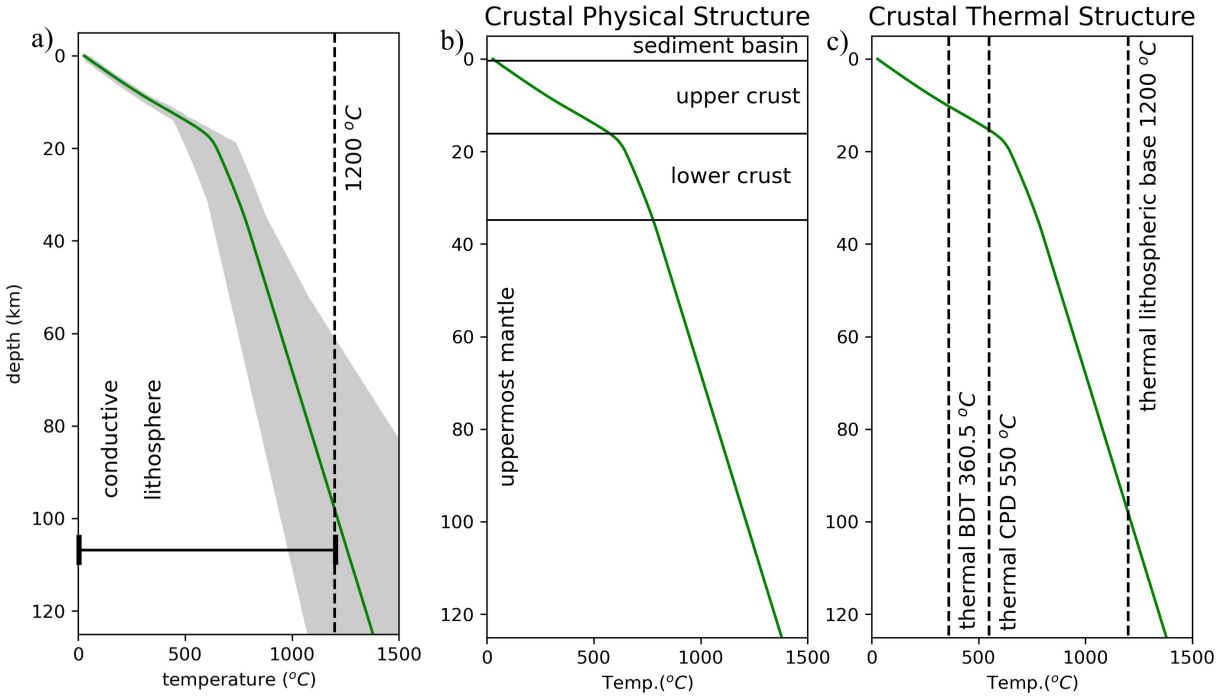

Figure 6. (a) Regional geotherms in Northern Thailand, grey lines representing all estimated geotherms with the green line as the average and the conductive region within the thermal limit of 1200 °C. (b) Crustal physical structure derived from the average output of the partitioned models. (c) Crustal thermal structure indicating the thermal brittle-ductile transition (BDT) at 360.5 °C, the Curie point depth (CPD) at 550 °C, and the thermal lithosphere base at 1200 °C.

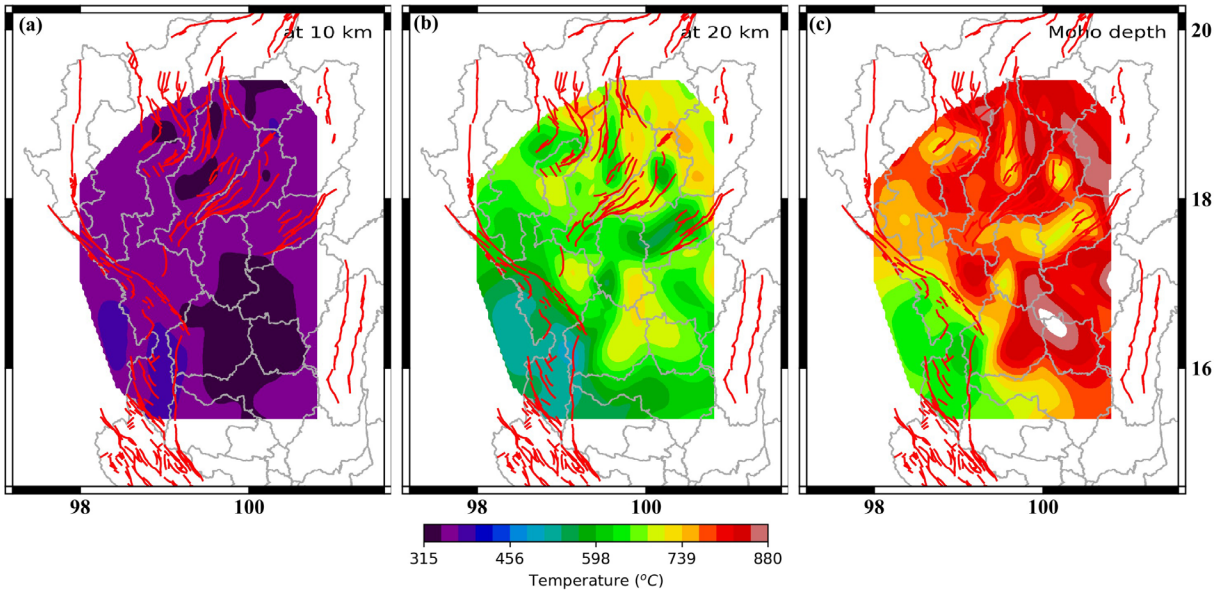

Figure 7. Temperature distributions at (a) 10 km, (b) 20 km, and (c) the Moho boundary derived from the modelled geotherms.

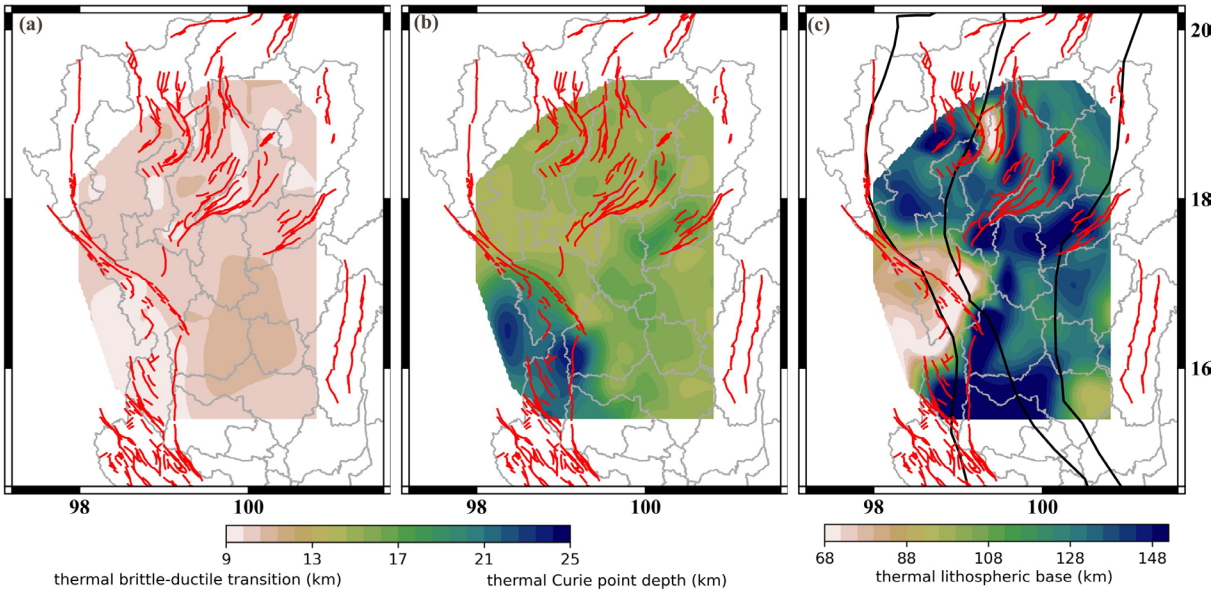

Figure 8. The results of thermal boundaries include the depth of thermal BDT at 360.5 °C (a), the depth of thermal CPD at 550 °C (b), and the depth of thermal lithospheric base at 1200 °C (c).

The thermal CPD tends to be shallower than the global thermal reference, while the thermal lithospheric base on average falls within the global thermal lithospheric model ranges but is slightly deeper than the SEA model. These variations result from the different constraints used in the global model and the different methods utilized in the SEA model. On the other hand, our model aims to provide a more localized representation for Northern Thailand while maintaining an average trend with respect to both previous models.

From Fig. 8a, the thermal BDT coincides with certain brittle shear zones, notably shallower around the suture zones (Nan-Uttaradit Suture and Chiang Mai-Chiang Rai Suture) and deeper in the basins. Figure 8b illustrates the thermal CPD deeper around the southwestern region where ST meets with the Inthanon Zone and Nan-Uttaradit Suture Zone. Figure 8c presents the thermal lithospheric base shallower in the western region and a small area in the northern province, reaching its greatest depth around the junction of the ST and Inthanon Zone in the southwest. A noteworthy observation is that the shallow region in the thermal lithospheric base in the northern part of the study area requires further investigation. This geological activity aligns with the relatively high heat flow and thermal conductivity observed in Fig. 4.

The crossplots (Fig. 9) show that the depth of basin sediment-basement rock aligns with the thermal BDT, while the upper-lower crust boundary inversely correlates with the thermal CDP. This observation suggests that regions

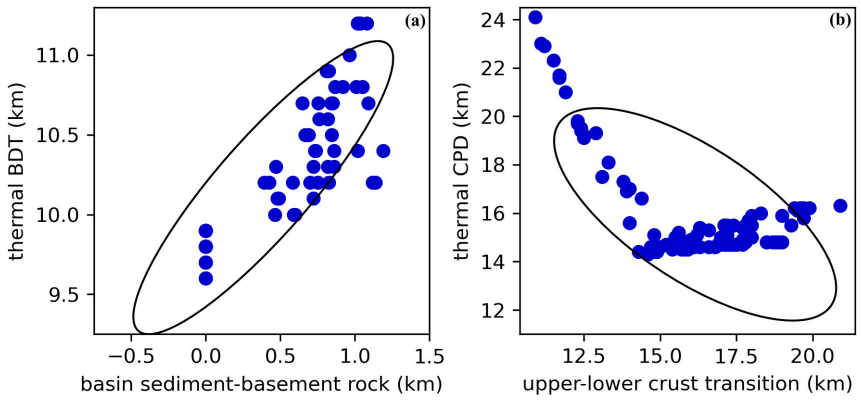

Figure 9. The crossplot between (a) the depth of basin sediment-basement rock versus thermal BDT, and (b) the upper-lower crust boundary and thermal CDP.

with thicker basin sediment tend to have deeper thermal BDT. Conversely, areas with a shallower upper-lower crust boundary tend to have a deeper thermal CPD (Fig. 9b). These findings support the idea that the radiogenic upper crust significantly influences crustal temperature (Hasterok and Chapman, 2011; Furlong and Chapman, 2013) in this region.

4. Shear zone model

This study employs the classic Christmas tree model to exemplify the mechanical behavior of Northern Thailand's crust. This model incorporates a quasi-elastic assumption in the shallow brittle zone and applies a wet quartzite flow law for deeper ductile behavior. Crustal heat flow variations are introduced to simulate both colder (70 – 20% mW m^{-2}) and hotter (70 + 20% mW m^{-2}) geothermal conditions, aiming to clarify the relationship between differential stress, temperature, and regional geothermal condition in Northern Thailand. The resulting geotherms are illustrated in Fig. 10.

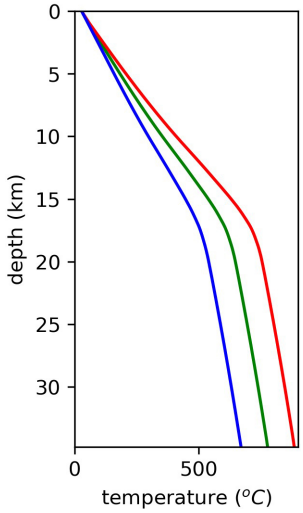

Figure 10. Variation of radiogenic-crustal-basal heat flow (q_B), 70 ± 20% mW m^{-2}, in Northern Thailand's geotherms. Blue line refers to cold geotherm, while red line is hot geotherm. Green line is an average regional geotherm in Northern Thailand.

The point where shallow earthquakes terminated is typically identified within a specific temperature range, representing the transition from brittle to ductile behavior. This range, known as quartz-dominant ductility, falls between 300 °C and 450 °C, corresponding to the ductility temperature of quartz-feldspar composition (Sibson, 1984; Scholz, 1988; Fagereng, 2013; Wehrens et al., 2016). The upper crust is usually assumed to be average quartz rheology, allowing the use of quartzite flow laws to explain flow behavior (e.g., Thompson et al., 2001).

Among various flow laws, the one developed by Hirth et al. (2001) was chosen, particularly suited for relatively low temperatures (up to 350 °C). Meanwhile, the thermal BDT in Northern Thailand was approximately defined at a temperature of 360.5 °C, where the quartz flow onset occurs, marking the transition from microcracks to uniform dislocations (Scholz, 1988).

The rheological properties of quartzite were analyzed using flow law equation (Hirth et al., 2001):

$$\dot{\varepsilon} = A f_{H_2O}^{m} (\sigma_1 - \sigma_3)^n \exp(-Q/RT) \tag{5}$$

where $\dot{\varepsilon}$ refers to strain rate (s^{-1}), A is a material parameter (MPa s^{-1}), f_{H_2O} is water fugacity, a measure of water potential in the form of adjusted pressure (MPa), m is water fugacity exponent, $\sigma_1 - \sigma_3$ is differential stress (MPa),

n is stress exponent, Q is activation energy (kJ mol^{-1}), R is ideal gas constant (8.314 J K^{-1}mol^{-1}), and T represents absolute temperature (K). Strain rate values ranging from 10^{-15} s^{-1} to 10^{-11} s^{-1} were also considered reasonable for crustal rock (Fagereng, 2013; Behr and Platt, 2014).

BDT temperatures under different geothermal conditions were then mapped onto these quartzite flow laws. It is important to note that σ_1 and σ_3, the greatest and least principal stresses, respectively, are considered to act in a plane normal to the shear zone.

In the brittle shear zone, rocks are assumed to behave as quasi-elastic particles, allowing the application of the linear frictional failure criterion proposed by Sibson (1974) and Hauksson and Meier (2019):

$$(\sigma_1 - \sigma_3)(z) = \alpha\rho(z)gz(1-\lambda) \tag{6}$$

where $\sigma_1 - \sigma_3$ represents the differential stress (MPa), α is a constant that depends on faulting type and frictional coefficient, ρ is the average rock density at depth shallower than z (g m^{-3}), g is the gravitational constant (m s^{-2}), and λ is pore fluid factor. The study employs the frictional law to establish a linear relationship between the differential stress and depth. Additionally, the thermal gradient is assumed to be equal to the ratio of BDT temperature (°C) to the average BDT depth (km).

Figure 11 depicts shear zone models under varying geothermal conditions (cold to hot). The model provides insight into the differential stress distribution along the shear plane, offering understanding of the mechanical behavior of the crust in response to temperature variations.

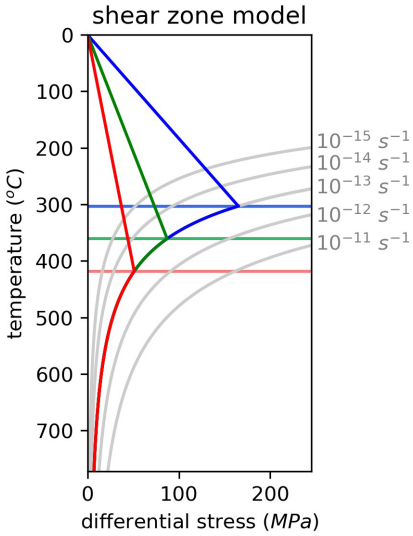

Figure 11. The shear zone models of cold (blue line) to hot (red line) geotherm. Green line is for regional geotherm.

This study extends its investigation of shear zone models by introducing variations in strain rate, offering insight into the dynamic behavior of shear zones in Northern Thailand. The analysis considers a range of strain rates from 10^{-15} s^{-1} to 10^{-12} s^{-1} (Violay et al., 2017), with a capped maximum shear stress of 120 MPa or equivalent differential stress of 240 MPa from the study of major shear zones by Behr and Platt (2014). The results are summarized in Table 1, presenting variation in heat flow, temperature, and differential stress.

The variation analysis explores adjustments in heat flow, temperature, and differential stress. Temperature adjustments within approximately ±16% of regional geotherm, corresponding to variation in heat flow from colder to hotter regions, reveal fluctuations in differential stress about +90% for colder geotherm and −41% for hotter geotherm compared to the regional result. Notably, for colder geotherm, the maximum strain rate slightly exceeded 10^{-13} s^{-1}, while for regional geotherm fell around 10^{-12} s^{-1}, and for hotter geotherms, a higher value was observed.

Table 1. The variation results in heat flow and strain rate.

BDT	Heat flow ($mW\,m^{-2}$)		
Temperature (°C)	56 (−20%)	70	84 (+20%)
Strain rate (s^{-1})	303.0 (−15.95%)	360.5	418.1 (+15.98%)
	Differential stress (MPa)		
10^{-15}	52.3 (+90.18%)	27.5	16.2 (−41.09%)
10^{-14}	92.9 (+89.59%)	49.0	28.7 (−41.43%)
10^{-13}	165.3 (+89.78%)	87.1	51.1 (−41.33%)
10^{-12}	—	154.9	90.8 (−41.38%)

The study emphasizes the significance of BDT in the middle crustal layer, influenced by lithology, strain rate, grain size, water content, and temperature (Sibson, 1984; Imber et al., 2001; Ellis and Stöckhert, 2004; Wehrens et al., 2016). Theoretical strength envelopes based on flow law rheology suggest that BDT depth correlates with strain rate and inversely correlates with heat flow (Sibson, 1984). Shallower BDT (hotter geotherm) is indicative of weaker crust, deforming more rapidly (Zuza and Cao, 2020; Fernández-Lozano et al., 2021). The lower strain rate would reduce flow stress (Meyer et al., 2019) and it responds to deeper BDT (colder geotherm).

Shear zone rocks can be approximately categorized into granular flow and/or brittle sliding (150-300 °C), brittle-ductile interplay (300-350 °C), and ductile flow (>350 °C) (Scholz, 1988; Fagereng and Toy, 2011). The rheological studies suggest that BDT temperatures may not distinctly separate brittle and ductile behavior, potentially leading to a smoothed differential stress profile (Fagereng and Beall, 2021).

The previous studies attribute the relatively weak major shear zone to high pore fluid pressure, dynamic weakening, and low coefficients of friction. These mechanisms, possibly temperature and depth dependent, could cease at around the BDT (Behr and Platt, 2014). If frictional/brittle sliding at low shear stress were possible, shear zones would deform through this mechanism instead of transitioning into dislocation creep at high shear stress (Imber et al., 2001). However, these attributions require further study beyond the scope of this paper.

The analysis of Northern Thailand reveals a failure limit up to 26 km in deep crust, surpassing the regional average upper-lower crust transition (16.15 km). However, 95% of regional earthquake nucleation terminates at depth less than 10.2 km (the regional average BDT), suggesting the presence of localized weak shear zones extending into the lower crust. These zones allow brittle failure at significantly greater depth than expected for dry and strong crust (Fagereng and Beall, 2021; Stevens et al., 2021). Further studies should focus on these localized zones to enhance understanding, considering non-uniform distribution of earthquakes around the study area.

5. Geothermal potential from hot dry rock (HDR)

The study evaluates the geothermal potential in Northern Thailand using hot dry rock (HDR) systems, focusing on temperature distribution at depth of 3.5 km, 5.5 km, and 9.5 km. The findings are presented in Fig. 12 providing insights into low-grade, economic-grade, and high-grade HDR potential (Tester et al., 2006; Jiang et al., 2016) across the region.

– Low-grade HDR potential (Fig. 12a): Areas with temperatures at least 120 °C are considered to have low-grade potential. Mountain ranges and some parts of the Chao Praya Floodplain, except Phitsanulok Basin, exhibit low-grade potential. Depths shallower than 3.5 km were not considered because their temperatures do not reach the 120 °C.

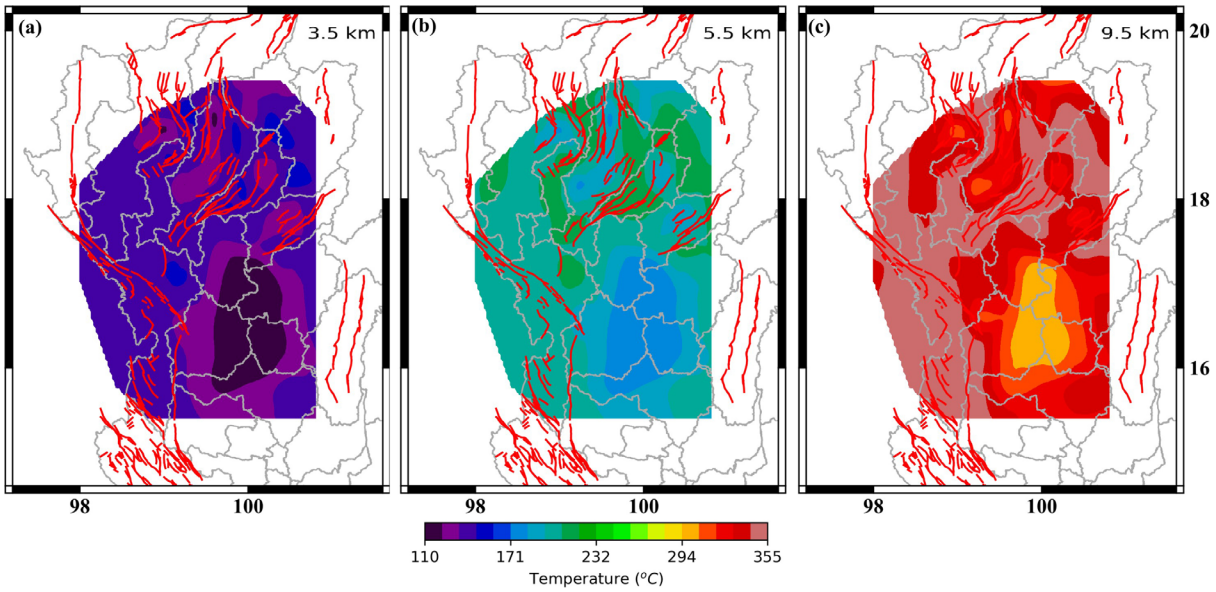

Figure 12. Temperatures at depth shown 3.5 km (a), 5.5 km (b), and 9.5 km (c) representing examples of low-grade, economic-grade, and high-grade HDR potentials, respectively.

- Economic grade HDR potential (Fig. 12b): Economic-grade potential is indicated by temperatures of at least 150 °C at a depth 5.5 km. The low-grade potential area remains noteworthy at this depth, with expanding potential provinces around the study area, including the basins.
- High-grade HDR potential (Fig. 12c): Higher-grade potential, characterized by temperatures of at least 250 °C. A depth of 9.5 km, it is most prominent in Western Thailand.

A pivotal finding is the significant expansion of HDR potential with increasing depth. At 5.5 km and 9.5 km depth, the entire area progressively transitions to moderate-grade and high-grade HDR potential, emphasizing the importance of considering carrying depths for a comprehensive geothermal resource evaluation.

The possible correlation between geothermal sources and granitic provinces in Fig. 13, as outlined by Cobbing et al. (1986) and Nachtergaele et al. (2020), could add a layer to our understanding of HDR distribution. Tak City aligns with Migmatite Complex Granite and the Northern Thailand Granite, which extends to the northern region. Additionally, the Eastern Granite to the east of Tak City and the east of the region highlights the possible influence of granitic composition on geothermal potential. These alignments could exemplify how the granitic composition of the crust can impact geothermal resources.

This study also estimates the theoretical stored heat content (Q_{block}) in exajoules (EJ) for different depth sections ranging from 3.5 km to 9.5 km in Northern Thailand. The Q_{block} is then converted into the thermal energy in terawatt hours (TW hr), providing an overview of the potential HDR thermal energy in the study area.

The Q_{block} is calculated using the formula:

$$Q_{block} = \rho c_p V_{block} \Delta T \tag{7}$$

where the density of rock (ρ) is in kg m^{-3}, specific heat capacity c_p is in J kg^{-1} °C^{-1}, the volume of rock (V_{block}) is in m^3 unit, and different temperatures from the surface (ΔT) is in °C.

As a reasonable approximation, the following values are typically assumed based on the works of Blackwell et al. (2006), and Tester et al. (2006): $\rho \sim 2550$ kg m^{-3} and $c_p \sim 1000$ J kg^{-1} °C^{-1}, V_{block} is calculated by multiplying the considered area by 1 km depth. The ΔT is calculated as the difference between the depth temperatures and the surface temperature by assuming it to represent the theoretically cooled-down temperature of the rock volume. Figure 14 summarizes the estimated stored heat content and the corresponding conversion to thermal energy potential at different depths.

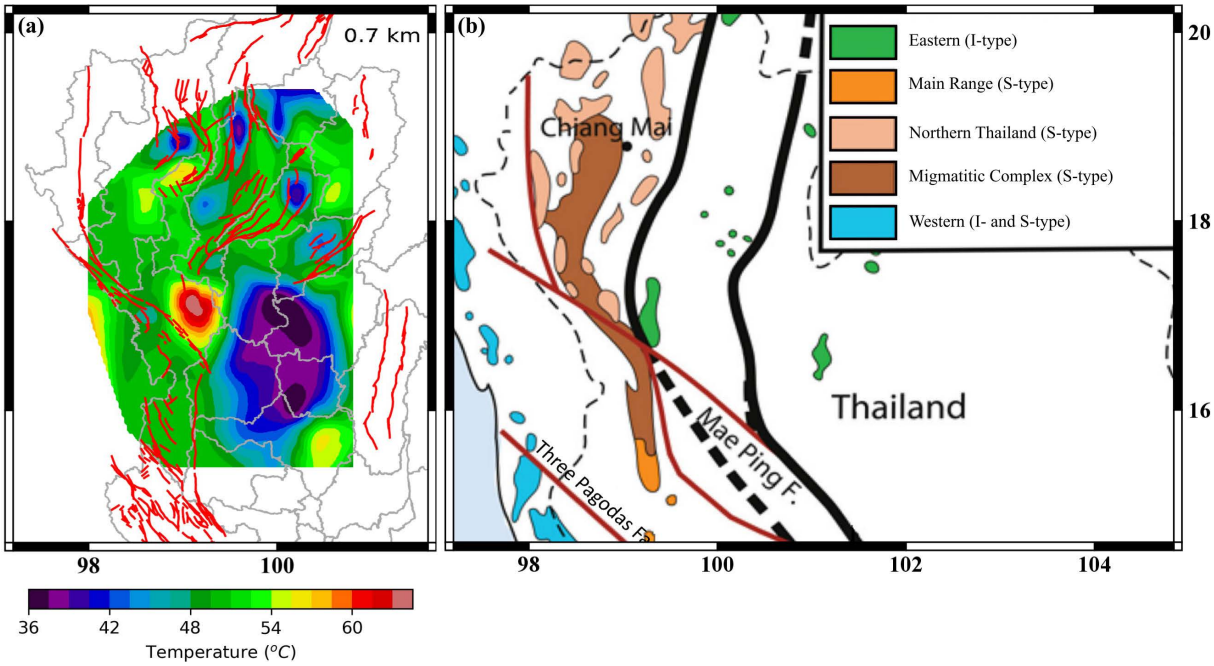

Figure 13. (a) Temperature at the depth of 0.7 km and (b) Northern Thailand's granitic provinces modified from Nachtergaele et al. (2020).

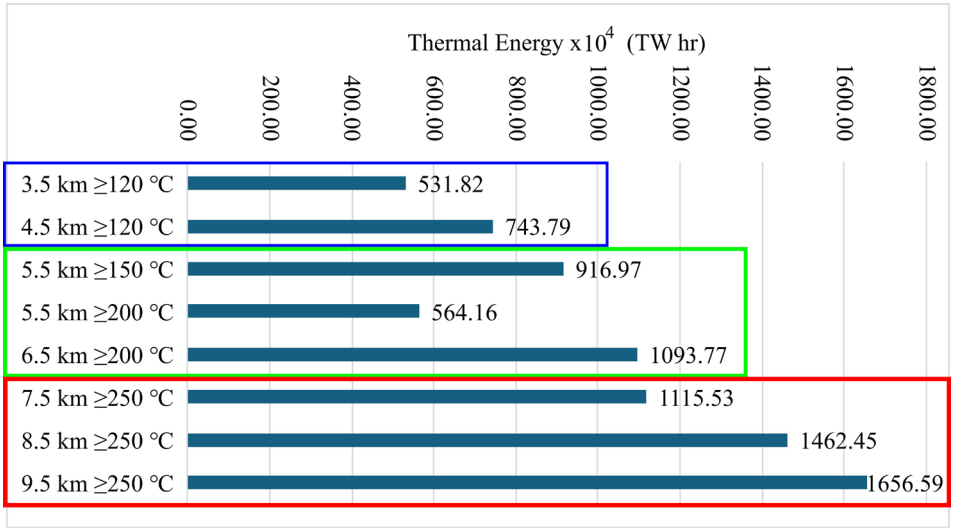

It is important to note that 1 EJ = 277.78 TW hr and 1 EJ = 1018 J.

Figure 14. The thermal energy in TW hr of each depth and temperature from low-grade (blue rectangle), economic-grade (green rectangle), and high-grade (red rectangle) potentials of geothermal energy in Northern Thailand.

Furthermore, the analysis of crustal thermal gradients in the study area, involving temperature averages at depth, has revealed significant observations, as illustrated in Fig. 15. At 10 km (Fig. 15a), the result indicates that hot springs are predominantly aligned with mountain range characterized by relatively high crustal thermal gradient. At 20 km (Fig. 15b), in contrast, the result is a notable shift in crustal thermal gradient, with some locations that previously exhibited low thermal gradients now demonstrate relatively high values and vice versa. This shift is attributed to the influence of deeper heat sources.

The ratio of crustal thermal gradient at the thermal brittle-ductile transition (thermal BDT) to the thermal Curie point depth (thermal CPD) marks as temperature reference boundaries (Fig. 15c). Preliminary ratio analysis suggests

that most hot springs are fed by deep heat sources, except in western areas and around Nan-Uttaradit Suture as shown in Fig 15c. The dominance of deep heat sources, as evidenced by slightly low ratio of BDT-to-CPD thermal gradient, emphasizes the importance of deep thermal structure processes in influencing temperature.

These findings contribute to our understanding of the factors influencing crustal thermal gradients in Northern Thailand. The interplay between shallow and deep heat sources adds complexity to the thermal landscape, providing insights into geothermal energy exploration of the region.

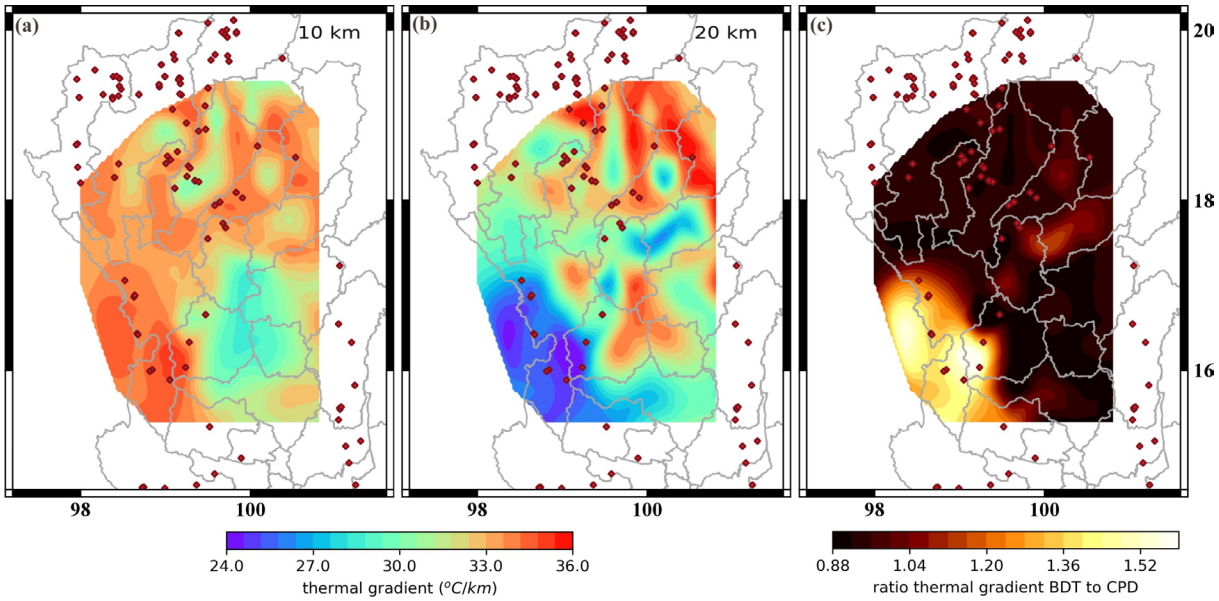

Figure 15. Thermal gradient averaged from temperature at 10 km (a) and 20 km (b). (c) ratio of thermal gradient at BDT to CPD. Hot spring locations (DMR, 2023a) are shown in red diamonds.

6. Calculation uncertainties

The estimation of 102 geotherms in Northern Thailand involves various assumptions and methodologies. Understanding these uncertainties is crucial for interpreting the results. The following points outline the key assumptions made in this study:

1) Extreme parameter values could have been influenced by borehole conditions, such as frictional heat, drilling mud, groundwater circulation. To overcome these, statistical analysis was applied to constrain these values,
2) The thermophysical parameters might not precisely align with considered grid, the regression based on k-nearest neighbors' approach was used to map parameters,
3) The potential lateral errors arising in the 1-D vertical study approach were acknowledged,
4) Local geology units were simplified into distinct categories,
5) The thermal brittle-ductile transition (thermal BDT) is assumed to coincide with the seismogenic base where the seismic activity's confidence interval cut off at 95% (cutoff depth 95; D95),
6) Since the uneven distribution of earthquakes across the area, D95 was treated as regional value rather than being specific to local shear segments,
7) The thermal brittle-ductile transition (thermal BDT), thermal Curie point depth (thermal CPD), and the thermal lithospheric base were assumed to maintain temperature consistent (360.5 °C, 550 °C, and 1200 °C, respectively),
8) BDT might be treated as a diffuse zone rather than a sharp boundary in these models. This recognition aims to align more closely with the actual nature of BDT,
9) Shear zone models were based solely on quartzite flow law, although it is acknowledged that the crustal rocks are polycrystals,

10) The uppermost part of Northern Thailand was not included in the study area, according to Siangpipop (2022). Some regions showed promisingly high thermal gradients in previous studies. Due to these limitations, the underestimation of Q_{block} for this region was acknowledged,
11) In practice, HDR exploitation is limited to some potential locations. The practical amount of reserve energy for economic purposes may be much lower than this theoretical estimated potential.

These assumptions provide a foundation for geothermal estimation, but they introduce uncertainties. Since these assumptions are simplified relative to real conditions, they primarily serve to facilitate this approximation of possible outcome for the region.

For example, the assumption of constant temperature at each temperature boundary does not fully reflect the mechanical BDT, as a temperature boundary – such as the Moho – can fall within a broad range (Sibson, 1977). Additionally, the assumption is primarily considered the effects of temperature and pressure on rheology, while overlooking other important factors, such as fluid pressure, mineralogy, and stress regime. Similarly, the assumption of quartz rheology introduces potential inaccuracies, as the actual rock composition at this depth in Northern Thailand may include various lithologies, leading to quantitative errors in the analysis.

Ultimately, the stored heat content should be regarded as a theoretical estimate rather than an absolute value. These values are derived from simplified lithologies in the study area. Furthermore, the depth and geometry of the different layers composing the crust are crucial for the success of longterm geothermal reservoir production.

One approach to evaluating conduction-dominant geothermal systems is by analyzing the ratio of porosity to permeability. Faults and fracture zones can enhance permeability at greater depths, thereby improving geothermal play systems (Moeck, 2014).

Therefore, users and researchers should consider these factors when interpreting the results and assessing their practical applicability in the context of geothermal resource exploration and utilization in Northern Thailand.

7. Sensitivity test

The sensitivity test evaluates how variations in initial parameters affect the geotherms equation, providing insight into the stability and reliability of the model. By examining fluctuations in thermal and seismic properties, we can assess how changes in mantle conductivity, heat flow, and shear wave velocity influence temperature distribution of thermal lithosphere. This analysis is crucial for refining geotherm models, identifying potential sources of error, and ensuring robust predictions in geophysical studies.

Thermal properties

- Lower crust thermal conductivity: 2.57 W/mK (Range: 2.44-2.7 W/mK)
- Mantle thermal conductivity: 4.0 W/mK (Range: 3.8-4.2 W/mK)
- Reduced heat flow: 70 mW/m^2 (Range: 66.5-73.5 mW/m^2)
- Thermal lithosphere thickness adjustment
  - Standard: 106.87 km
  - Variability: −1.4% to +1.3%/−3.8% to +3.3%/+3.8% to −3.9%, respectively.

Seismic properties

- Shear wave velocity (upper crust): 3.41 km/s (Range: 3.24-3.58 km/s)
- Shear wave velocity (lower crust): 3.71 km/s (Range: 3.52-3.9 km/s)
- Thermal lithosphere thickness adjustment
  - Standard: 106.87 km
  - Variability: −3.6% to +1.3%/−2.4% to +1%, respectively.

8. Conclusions

This research has advanced our comprehension of the thermal and structural characteristics of Northern Thailand's crust through synthesizing existing studies and introducing new investigations. Analyzes of thermophysical

data have led to the development of 1-D partitioned geotherms. These geotherms have facilitated the identification of crucial thermal boundaries, including the thermal brittle-ductile transition (thermal BDT), the thermal Curie point depth (thermal CPD), and the base of the thermal uppermost mantle or thermal lithospheric base. Furthermore, this work highlights the significance of heat flow value and strain rate on the differential stress within the shear zone of the Northern Thailand, underscoring the need for further investigation.

The research also identifies the region as having at least low-grade potential hot dry rock (HDR). The estimated theoretical regional stored heat content opens possibilities for sustainable and eco-friendly energy development, with potential applications in enhanced geothermal systems (EGS). Furthermore, the research addresses the correlation between hot spring locations and the crustal thermal gradient, suggesting different heat sources from both shallow and deep origins.

Acknowledging inherent uncertainties, the study provides a foundation for future investigations, highlighting the need for nuanced consideration of geological units, tectonic settings, and the environmental issues in the region. While setting the stage for further research, this work could help pave the way for understanding Northern Thailand's crustal thermal structure for hazard assessment and sustainable energy development.

Data availability statement.

- The global heat flow database is maintained by the International Heat Flow Commission (IHFC) of International Association of Seismology and Physics of the Earth's Interior (IASPEI). Data can be downloaded at: https://ihfc-iugg.org/ (last accessed May 2023)
- The local earthquake catalog is collected by the Earthquake Observation Division of Thai Meteorological Department (TMD). Data can be obtained at: https://earthquake.tmd.go.th/ (last accessed November 2022).

Declaration of Competing Interest. The authors declare the absence of any conflicts of interest related to the research. There are no financial, personal, or professional relationships that could be perceived as influencing the research outcomes.

Acknowledgements. We would like to express our sincere appreciation and gratitude to the National Science and Technology Development Agency (NSTDA), Thailand, for the financial support, which made this research possible. Their funding has greatly contributed to the progress and success of this study. We would also like to express our gratitude to the International Heat Flow Commission (IHFC), Thai Meteorological Department (TMD) and Department of Mineral Resources (DMR) for providing the catalogues of data used in this research. Moreover, we would like to extend our appreciation to the Department of Geological Sciences at Chiang Mai University for their support throughout this research. Special thanks to A. Yawichai for his technical assistance and S. S. Gourlay for her feedback on reviewing this work. This work drew significant inspiration from the studies conducted by Pollack and Chapman (1977), Thienprasert and Raksaskulwong (1984), Artemieva (2006), and Behr and Platt (2014), Jiang et al. (2016). Finally, I sincerely thank the anonymous reviewers for their thoughtful comments and constructive suggestions, which greatly improved the quality and clarity of this work.

References

Aghahosseini, A. and C. Breyer (2020). From hot rock to useful energy: A global estimate of enhanced geothermal systems potential, Appl. Energ., 279, 115769, doi:10.1016/j.apenergy.2020.115769.

Artemieva, I. (2011). Lithosphere: an interdisciplinary approach, Cambridge University Press, Cambridge. doi:10.1017/CBO9780511975417.

Artemieva, I. M. (2006). Global 1×1 thermal model TC1 for the continental lithosphere: implications for lithosphere secular evolution, Tectonophysics, 416, no. 1-4, 245-277, doi:10.1016/j.tecto.2005.11.022.

Artemieva, I. M. and W. D. Mooney (2001). Thermal thickness and evolution of Precambrian lithosphere: A global study, J. Geophys. Res-Solid Earth, 106, B8, 16387-16414, doi:10.1029/2000JB900439.

Behr, W. M. and J. P. Platt (2014). Brittle faults are weak, yet the ductile middle crust is strong: Implications for lithospheric mechanics, Geophys. Res. Lett., 41, 22, 8067-8075, doi:10.1002/2014GL061349.

Blackwell, D. D., P. T. Negraru and M. C. Richards (2006). Assessment of the enhanced geothermal system resource base of the United States, Natural Resources Research, 15, 283-308, doi:10.1007/s11053-007-9028-7.

Bonner, J. L., D. D. Blackwell and E. T. Herrin (2003). Thermal constraints on earthquake depths in California, Bull. Seismol. Soc. Am., 93, 6, 2333-2354, doi:10.1785/0120030041.

Caristan, Y. (1982). The transition from high temperature creep to fracture in Maryland diabase, J. Geophys. Res-Solid Earth, 87, B8, 6781-6790, doi:10.1029/JB087iB08p06781.

Chamorro, C. R., J. L. García-Cuesta, M. E. Mondéjar and M. M. Linares (2014). An estimation of the enhanced geothermal systems potential for the Iberian Peninsula, Renew. Energ., 66, 1-14, doi:10.1016/j.renene.2013.11.065.

Chapman, D. (1986). Thermal gradients in the continental crust, Geological Society, London, Special Publications, 24, 1, 63-70, doi:10.1144/GSL.SP.1986.024.01.0.

Charusiri, P. (2002). Geotectonic evolution of Thailand: a new synthesis, J. Geol. Soc. Thai, 1, 1-20.

Chiarabba, C. and P. De Gori (2016). The seismogenic thickness in Italy: constraints on potential magnitude and seismic hazard, Terra Nova, 28, 6, 402-408, doi:10.1111/ter.12233.

Cobbing, E., D. Mallick, P. Pitfield and L. Teoh (1986). The granites of the Southeast Asian tin belt, J. Geol. Soc. London, 143, 3, 537-550, doi:10.1144/gsjgs.143.3.05.

Craig, T. and J. Jackson (2021). Variations in the seismogenic thickness of East Africa, J. Geophys. Res-Solid Earth, 126, 3, e2020JB020754, doi:10.1029/2020JB020754.

Cull, J., S. Y. O'Reilly and W. Griffin (1991). Xenolith geotherms and crustal models in eastern Australia, Tectonophysics, 192, 3-4, 359-366, doi:10.1016/0040-1951(91)90109-6.

Dessai, A. G. (2020). The Lithosphere Beneath the Indian Shield: A Geodynamic Perspective, 20, Springer Nature, ISSN 1876-1690.

DMR, Department of Mineral Resources (2018). Report of characteristics of radioactivity data and magnetic field intensity data in the application of Thailand geological survey (in Thai), Department of Mineral Resources.

DMR, Department of Mineral Resources (2023a). Report of hot spring (in Thai), Department of Mineral Resources.

DMR, Department of Mineral Resources (2023b). Report of active fault zones (in Thai), Department of Mineral Resources.

Ellis, S. and B. Stöckhert (2004). Elevated stresses and creep rates beneath the brittle-ductile transition caused by seismic faulting in the upper crust, J. Geophys. Res.-Solid Earth, 109, B5, doi:10.1029/2003JB002744.

Fagereng, Å. (2013). Fault segmentation, deep rift earthquakes and crustal rheology: Insights from the 2009 Karonga sequence and seismicity in the Rukwa-Malawi rift zone, Tectonophysics, 601, 216-225, doi:10.1016/j.tecto.2013.05.012.

Fagereng, Å. and V. G. Toy (2011). Geology of the earthquake source: an introduction, Geological Society, London, Special Publications, 359, 1, 1-16, doi:10.1144/SP359.1.

Fagereng, Å. and A. Beall (2021). Is complex fault zone behaviour a reflection of rheological heterogeneity?, Philos. T. R. Soc. A, 379, 2193, 20190421, doi:10.1098/rsta.2019.0421.

Fernández-Lozano, J., F. Martín-González and G. De Vicente (2021). New Insights into the Lateral-Strength Variations and Depth to the Brittle-Ductile Transition Zone in NW Iberia, Tectonics, 40, 2, e2020TC006493, doi:10.1029/2020TC006493.

Förster, A., S. Fuchs, H.-J. Förster and B. Norden (2021). Ambiguity of crustal geotherms: a thermal-conductivity perspective, Geothermics, 89, 101937, doi:10.1016/j.geothermics.2020.101937.

Fuchs, S., F. Neumann, B. Norden, G. Beardsmore et al. (2023). The Global Heat Flow Database: Update 2023., V. 1. GFZ Data Services. doi:10.5880/fidgeo.2023.008.

Furlong, K. P. and D. S. Chapman (2013). Heat flow, heat generation, and the thermal state of the lithosphere, Annu. Rev. Earth P.L. SC., 41, 385-410, doi:10.1146/annurev.earth.031208.100051.

Hall, R. and C. K. Morley (2004). Sundaland Basins, in: Continent-ocean interactions within East Asian marginal seas, P. Clift, W. Kuhnt, P. Wang, D. Hayes (eds.), Geophysical Monograph Series 149, 55-85, doi:10.1029/GM149.

Hansen, B. T. and K. Wemmer (2011). Age and evolution of the basement rocks in Thailand, The Geology of Thailand. Geological Society, London, 19-32, doi:10.1144/GOTH.2.

Hansen, B. T., K. Wemmer, P. Putthapiban, I. C. Kleinhanns et al. (2014). Do U/Pb-SHRIMP dating and Pb stepwise leaching (PbSL) analyses confirm the lack of precambrian basement outcrops in Thailand?, Open J. Geol., 4, 10, 505-517, doi:10.4236/ojg.2014.410037.

Hasterok, D. and D. Chapman (2011). Heat production and geotherms for the continental lithosphere, Earth Planet. Sci. Lett., 307, 1-2, 59-70, doi:10.1016/j.epsl.2011.04.034.

Hauksson, E. and M.-A. Meier (2019). Applying depth distribution of seismicity to determine thermo-mechanical properties of the seismogenic crust in Southern California: comparing lithotectonic blocks, Pure. Appl. Geophys., 176, 3, 1061-1081, doi:10.1007/s00024-018-1981-z.

Hirth, G., C. Teyssier and J. W. Dunlap (2001). An evaluation of quartzite flow laws based on comparisons between experimentally and naturally deformed rocks, Int. J. Earth Sci., 90, 77-87, doi:10.1007/s005310000152.

Hutchison, C. S. (2014). Tectonic evolution of Southeast Asia, Bulletin of the Geological Society of Malaysia, 60, 1-18, doi:10.7186/bgsm60201401.

Imber, J., R. Holdsworth, C. Butler and R. Strachan (2001). A reappraisal of the Sibson-Scholz fault zone model: The nature of the frictional to viscous ("brittle-ductile") transition along a long-lived, crustal-scale fault, Outer Hebrides, Scotland, Tectonics, 20, 5, 601-624, doi:10.1029/2000TC001250.

Jackson, I. and R. J. Arculus (1984). Laboratory wave velocity measurements on lower crustal xenoliths from Calcutteroo, South Australia, Tectonophysics, 101, 1-2, 185-197, doi:10.1016/0040-1951(84)90051-9.

Jennings, S., D. Hasterok and F. Lucazeau (2021). ThermoGlobe: extending the global heat flow database, Journal TBD.

Jiang, G., W. Li, W. Li, S. Rao, Y. Shi et al. (2016). Heat flow, depth-temperature, and assessment of the enhanced geothermal system (EGS) resource base of continental China, Environ. Earth Sci., 75, 22, 1-10, doi:10.1007/s12665-016-6238-5.

Lekuthai, T., R. Charusirisawad, and M. Vacher (1995). Heat flow map of the Gulf of Thailand, CCOP Technical bulletin, 25, 63-78.

Lythgoe, K., M. Muzli, K. Bradley, T. Wang et al. (2021). Thermal squeezing of the seismogenic zone controlled rupture of the volcano-rooted Flores Thrust, Sci. Adv., 7, 5, eabe2348, doi:10.1126/sciadv.abe2348.

Mareschal, J.-C. and C. Jaupart (2013). Radiogenic heat production, thermal regime and evolution of continental crust, Tectonophysics, 609, 524-534, doi:10.1016/j.tecto.2012.12.001.

Metcalfe, I. (2017). Tectonic evolution of Sundaland, Bulletin of the Geological Society of Malaysia, 63, 27-60. doi:10.7186/bgsm63201702.

Meyer, G. G., N. Brantut, T. M. Mitchell and P. G. Meredith (2019). Fault reactivation and strain partitioning across the brittle-ductile transition, Geology, 47, 12, 1127-1130, doi:10.1130/G46516.1.

MOE, Ministry of Energy (2018). the Alternative Energy Development Plan 2018-2037 (in Thai), Minister of Energy.

Moeck, I. S. (2014). Catalog of geothermal play types based on geologic controls, Renew Sustain Energy Rev., 37, 867-882, doi:10.1016/j.rser.2014.05.032.

Morley, C. and S. Chantraprasert (2022). Plume-related, syn-rift, Neogene volcanism, the interplay with structure in Thailand and comparison with the East African Rift, Ital. J. Geosci., 141, 3, 295-333, doi:10.3301/IJG.2022.24.

Nachtergaele, S. (2020). Cenozoic tectonic evolution of southeastern Thailand derived from low-temperature thermochronology, J. Geol. Soc. London, 177, 2, 395-411, doi:10.1144/jgs2018-167.

Nazareth, J. J. and E. Hauksson (2004). The seismogenic thickness of the southern California crust, Bull. Seismol. Soc. Am., 94, 3, 940-960, doi:10.1785/0120020129.

Noisagool, S. (2022). North and Western Thailand Regional Average Velocity model (personal communication).

Noisagool, S., S. Boonchaisuk, P. Pornsopin and W. Siripunvaraporn (2014). Thailand's crustal properties from tele-seismic receiver function studies, Tectonophysics, 632, 64-75, doi:10.1016/j.tecto.2014.06.014.

Okubo, Y. and T. Matsunaga (1994). Curie point depth in northeast Japan and its correlation with regional thermal structure and seismicity, J. Geophys. Res.-Solid Earth, 99, B11, 22363-22371, doi:10.1029/94JB01336.

Petkaew, P. (2015). 3D Shear Wave Velocity Model Across Thailand Using Surface Wave Inversion of Ambient Seismic Noise, MS Thesis, Chiang Mai University.

Petkaew, P. (2022). Surface wave tomography and assessing the uncertainty of ambient seismic noise data across Thailand, PhD Thesis, University of Leicester.

Pollack, H. N. and D. S. Chapman (1977). On the regional variation of heat flow, geotherms, and lithospheric thickness, Tectonophysics, 38, 3-4, 279-296, doi:10.1016/0040-1951(77)90215-3.

Price, N. A., S. E. Johnson, C. C. Gerbi, and D. P. West Jr (2012). Identifying deformed pseudotachylyte and its influence on the strength and evolution of a crustal shear zone at the base of the seismogenic zone, Tectonophysics, 518, 63-83, doi:10.1016/j.tecto.2011.11.011.

Raksaskulwong, M. and A. Thienprasert (1995). Heat flow studies and geothermal energy development in Thailand. In M. L. Gupta and M. Yamano (Eds.), Terrestrial heat flow and geothermal energy in Asia 129-144, Science Publ.

Rozalli, M., N. Mankhemthong, C. K. Morley, and P. Limtrakun, (2020). Indosinian Orogeny Structure in Ban Pong and Ban Hong Quarries, Chiang Mai and Lamphun Provinces, Northwestern Thailand, European Association of

Geoscientists and Engineers, 3rd Asia Pacific Meeting on Near Surface Geoscience and Engineering, Nov 2020, 2020, 1-5, doi:10.3997/2214-4609.202071055.

Rybach, L. (1976). Radioactive heat production in rocks and its relation to other petrophysical parameters, Pure Appl. Geophys., 114, 309-317, doi:10.1007/BF00878955.

Rybach, L. and G. Buntebarth (1984). The variation of heat generation, density and seismic velocity with rock type in the continental lithosphere, Tectonophysics, 103, 1-4, 335-344, doi:10.1016/0040-1951(84)90095-7.

Rychert, C. A., N. Harmon, S. Constable and S. Wang (2020). The nature of the lithosphere-asthenosphere boundary, J. Geophys. Res-Solid Earth, 125, 10, e2018JB016463, doi:10.1029/2018JB016463.

Schärmeli, G. (1979). Identification of radiative thermal conductivity of olivine up to 25 kbar and 1500 K, High-Pressure Science and Technology: Volume 1: Physical Properties and Material Synthesis/Volume 2: Applications and Mechanical Properties, Springer US, Boston, 1092-1106.

Schatz, J. F. and G. Simmons (1972). Thermal conductivity of Earth materials at high temperatures, J. Geophys. Res., 77, 35, 6966-6983, doi:10.1029/JB077i035p06966.

Schettino, A. (2014). Quantitative plate tectonics: Physics of the Earth-Plate Kinematics-Geodynamics, Springer, doi:10.1007/978-3-319-09135-8.

Scholz, C. (1988). The brittle-plastic transition and the depth of seismic faulting, Geol. Rundsch., 77, 319-328, doi:10.1007/BF01848693.

Siangpipop, S. (2022). Shear Wave Velocity Model by C1 and C2 Combination Using Ambient Seismic Noise Beneath Northern Thailand, MS Thesis, Chiang Mai University.

Sibson, R. H. (1974). Frictional constraints on thrust, wrench and normal faults, Nature, 249, 5457, 542-544, doi:10.1038/249542a0.

Sibson, R. (1977), Fault rocks and fault mechanisms, J Geol. Soc. London, 133, 3, 191-213, doi:10.1144/gsjgs.133.3.0191.

Sibson, R. H. (1984). Roughness at the base of the seismogenic zone: contributing factors, J. Geophys. Res.-Solid Earth, 89, B7, 5791-5799, doi:10.1029/JB089iB07p05791.

Sibson, R. H. (1986). Earthquakes and rock deformation in crustal fault zones, Annu. Rev. Earth. PL. SC., 14, 1, 149-175.

Stevens, V., R. Sloan, P. Chindandali, L. N. Wedmore et al. (2021). The entire crust can be seismogenic: Evidence from southern Malawi, Tectonics, 40, 6, e2020TC006654, doi:10.1029/2020TC006654.

Tadapansawut, T. (2012). Thailand crustal thickness estimation using joint inversion of surface wave dispersion and receiver functions, MS Thesis, Chiang Mai University.

Tanaka, A., Y. Okubo and O. Matsubayashi (1999). Curie point depth based on spectrum analysis of the magnetic anomaly data in East and Southeast Asia, Tectonophysics, 306, 3-4, 461-470, doi:10.1016/S0040-1951(99)00072-4.

Tester, J. W., B. J. Anderson, A. Batchelor, D. Blackwell et al. (2006). The future of geothermal energy, Massachusetts Institute of Technology, 358, ISBN: 0615134386.

Thienprasert, A. and M. Raksaskulwong (1984). Heat flow in northern Thailand, Tectonophysics, 103, 1-4, 217-233, doi:10.1016/0040-1951(84)90085-4.

Thompson, A., K. Schulmann, J. Jezek, V. Tolar (2001). Thermally softened continental extensional zones (arcs and rifts) as precursors to thickened orogenic belts, Tectonophysics, 332, 1-2, 115-141, doi:10.1016/S0040-1951(00)00252-3.

TMD, Thai Meteorological Department (2019). Report of annual temperature: Selected location by regions 2015-2019 (in Thai), Thai Meteorological Department.

TMD, Thai Meteorological Department (2021). Thailand's local earthquakes catalogue 2007-2021, Thai Meteorological Department.

Uchida, Y., K. Yasukawa, N. Tenma, Y. Taguchi et al. (2011). Subsurface temperature survey in Thailand for geothermal heat pump application, J. Geothermal Res. Soc. Japan, 33, 2, 93-98, doi:10.11367/grsj.33.93.

Violay, M., M. J. Heap, M. Acosta, and C. Madonna (2017). Porosity evolution at the brittle-ductile transition in the continental crust: Implications for deep hydro-geothermal circulation, Sci. Rep.-UK, 7, 1, 7705, doi:10.1038/s41598-017-08108-5.

Wehrens, P., A. Berger, M. Peters, T. Spillmann et al. (2016). Deformation at the frictional-viscous transition: Evidence for cycles of fluid-assisted embrittlement and ductile deformation in the granitoid crust, Tectonophysics, 693, 66-84, doi:10.1016/j.tecto.2016.10.022.

Wood, S. H., P. Kaewsomwang and F. S. Singharajwarapan (2018). Geologic framework of the Fang Hot Springs area with emphasis on structure, hydrology, and geothermal development, Chiang Mai Province, northern Thailand, Geothermal Energy, 6, 1, 1-51, doi:10.1186/s40517-017-0087-7.

Wright, T. J., J. R. Elliott, H. Wang and I. Ryder (2013). Earthquake cycle deformation and the Moho: Implications for the rheology of continental lithosphere, Tectonophysics, 609, 504-523, doi:10.1016/j.tecto.2013.07.029.

Wu, W.-N., Y.-T. Yen, Y.-J. Hsu, Y.-M. Wu et al. (2017). Spatial variation of seismogenic depths of crustal earthquakes in the Taiwan region: Implications for seismic hazard assessment, Tectonophysics, 708, 81-95, doi:10.1016/j.tecto.2017.04.028.

Yu, C., X. Shi, X. Yang, J. Zhao et al. (2017). Deep thermal structure of Southeast Asia constrained by S-velocity data, Mar. Geophys. Res., 38, 341-355, doi:10.1007/s11001-017-9311-x.

Zahirovic, S., M. Seton, and R. Müller (2014). The Cretaceous and Cenozoic tectonic evolution of Southeast Asia, Solid Earth, 5, 1, 227-273, doi:10.5194/sed-5-1335-2013.

Zuza, A. V. and W. Cao (2020). Seismogenic thickness of California: Implications for thermal structure and seismic hazard, Tectonophysics, 782, 228426, doi:10.1016/j.tecto.2020.228426.

***CORRESPONDING AUTHOR: Siriporn CHAISRI**,
Chiang Mai University, Department of Physics and Materials Science, Chiang Mai, Thailand
e-mail:siriporn.chaisri@cmu.ac.th